Large-Eddy Simulation of a Turbulent Reacting Liquid Flow

Takenobu Michioka and Satoru Komori
Dept. of Mechanical Engineering and Advanced Research Institute of Fluid Science and Engineering, Kyoto University, Kyoto 606-8501, Japan

DOI 10.1002/aic.10218
Published online in Wiley InterScience (www.interscience.wiley.com).

A subgrid-scale (SGS) model for the filtered reaction source term is presented to develop the large-eddy simulation (LES) of a nonpremixed, turbulent liquid flow with a moderately fast reaction. The SGS model is based on the SGS probability density function (PDF) and SGS conditional expectation. The SGS probability density function (SGS–PDF) is assumed to follow a beta distribution and a simple algebraic model for the SGS conditional expectation is developed using the filtered data obtained from the direct numerical simulation (DNS) of stationary isotropic liquid turbulence with a second-order chemical reaction. For a rapid reaction, the SGS–PDF model based on the conserved scalar is used as the SGS model. The LES based on these SGS models is applied to a liquid mixing layer flow downstream of a turbulence-generating grid with a chemical reaction, and the LES predictions of the mean concentration and concentration variance are directly compared with the previous measurements for both moderately fast and rapid reactions to examine the proposed SGS models. The results show that the predictions by the LES are in good agreement with the measurements and the present LES can well describe the diffusive–reactive process in a turbulent reacting liquid flow. © 2004 American Institute of Chemical Engineers *AIChE J,* 50: 2705–2720, 2004
Keywords: large-eddy simulation, subgrid-scale model, probability density function, direct numerical simulation, turbulent reacting liquid flow

Introduction

Turbulent reacting liquid flows are widely seen in many chemical reactors and environmental flows. Therefore, development of accurate numerical simulation of a turbulent reacting liquid flow is needed to aid in designing chemical reactors and in predicting turbulent diffusion of chemical pollutants in rivers and oceans. Time-averaged Navier–Stokes (N-S) and mass conservation equations have often been used for predicting velocity and concentration fields in practical chemical reactors. Application of this method to a turbulent reacting liquid flow requires accurate closure models for time-averaged reaction source term. However, this approach does not always give good agreement with the measurement of concentration fluctuations (Wang and Tarbell, 1993), although several closure models such as Toor's model (Toor, 1969), three environmental (3E) model (Ritchie and Tobgy, 1979), and Patterson's model (Patterson, 1981) have been proposed for the reaction source term. On the other hand, the most complete approach is the direct numerical simulation (DNS), which directly solves the N-S and mass conservation equations. However, it is difficult to adopt the DNS for a turbulent reacting liquid flow with high Reynolds and Schmidt numbers, because the minimum scale of the concentration fluctuation, that is, the Batchelor scale, is quite small compared to the Kolmogorov scale.

Large-eddy simulation (LES) is a very attractive tool for numerically simulating a turbulent reacting flow with high Reynolds and Schmidt numbers. Velocity and concentration at large scales [grid-scales (GS)] are computed directly from the

Present address of T. Michioka: Environmental Science Research Laboratory, Central Research Institute of Electric Power Industry, Abiko, Chiba 270-1194, Japan.
Correspondence concerning this article should be addressed to S. Komori at komori@mech.kyoto-u.ac.jp.

solutions of the filtered Navier–Stokes and mass conservation equations, and velocity and concentration fields at small scales [subgrid-scales (SGS)] are modeled to close the SGS stresses, SGS mass fluxes, and filtered reaction source term. Several models have been proposed to describe the SGS stresses and SGS mass fluxes. The most prominent model has been the Smagorinsky model (Smagorinsky, 1963). Germano et al. (1991), Lilly (1992), and Piomelli and Liu (1995) all proposed the dynamic SGS models for the SGS stresses and SGS mass fluxes, and the constants that appear in the Smagorinsky model have been computed dynamically, as a function of space and time. The dynamic modeling ideas may be useful in SGS modeling for a reacting flow, since the eddy diffusivity of mass changes depending the reaction (Komori et al., 1993a).

One of the major issues toward the development of the LES of a reacting flow is to use an adequate SGS model for the filtered reaction source term. Schumann (1989) and Sykes et al. (1992) applied the LES to a reacting atmospheric flow. In their simulations, the filtered reaction source term was approximated only in terms of the GS concentration and the effects of SGS concentration fluctuation were neglected. However, Riley et al. (1986) and Meeder and Nieuwstadt (2000) reported the importance of the SGS fluctuation correlation in the filtered reaction source term. Thus, it is essential to take the effects of the SGS concentration fluctuation into the LES of a turbulent reacting flow.

Germano et al. (1996) extended the Germano dynamic SGS model to a reacting flow. Although these models are attractive because of their simplicity, the constants appearing in these models seem to strongly depend on flow and reaction conditions and grid size for the computation. Cook and Riley (1998) proposed a steady laminar flamelet model for the filtered reaction source term. Pitsch and Steiner (2000) developed an unsteady laminar flamelet model. However, these laminar flamelet models cannot be easily applied to a turbulent reacting flow with the low Damköhler number such as the present moderately fast reaction case because the models are appropriate only for fairly large Damköhler numbers (Pierce, 2001). In these points these models may not be enough to be applied to an arbitrary turbulent reacting flow.

The conditional moment closure (CMC) method first proposed by Bilger (1993) has been applied to turbulent reacting flows. However, it is almost impossible to apply the CMC method to a practical reacting flow because the CMC method needs a huge computation time to solve the transport equations for the filtered concentrations, conditional on the mixture fraction. Instead of solving these transport equations, Baldyga (1994) determined the concentrations, conditional on the mixture fraction, by linearly interpolating the concentrations between the rapid reaction case and no reaction case. Unfortunately, the accuracy of the linear interpolation method in the LES has not been confirmed by comparing with any experimental data or DNS predictions. Recently, Bushe and Steiner (1999) developed an LES based on the CMC method. However, it should be noted that the CMC method is applicable only to a simple reacting flow with the homogeneity at least in one direction and not applicable to such a complicated flow in a practical chemical reactor with three-dimensional mean velocity or concentration field.

Gao and O'Brien (1993) proposed the SGS model based on the joint probability density function (PDF) of concentrations of two chemical species and derived a transport equation for the joint PDF. Colucci et al. (1998) and Jaberi et al. (1999) numerically solved the transport equation by means of a Lagrangian Monte Carlo procedure. Komori et al. (1991), Briens et al. (1995), and Van Dop (2001) developed Lagrangian stochastic models for the mixing of two reacting species. The PDF method has an advantage that any assumption for the reaction source term is not needed. However, the procedure needs some closure hypotheses for the diffusion terms, and it is not easy to apply to a practical three-dimensional reacting flow with complicated flow field. On the other hand, Cook and Riley (1994) proposed the beta assumed-PDF approximation, in which the concentrations at grid scales were directly solved using a conserved scalar approach. The conserved scalar approach is very advantageous for a rapid reaction but not for a moderately fast reaction because this approach becomes simple only when the timescale of the chemical reaction is sufficiently fast compared to that of the turbulent mixing.

Thus, simple and adequate SGS modeling for a turbulent reacting flow is still crucial. In addition, the previous models have been proposed only for a turbulent reacting air flow with the low Schmidt number, and therefore it is not clear whether the previous SGS models can be applied to a turbulent reacting liquid flow with the high Schmidt number, which is quite often seen in chemical reactors. Here it should be noted that it is of great practical importance in designing chemical reactors to develop simple SGS models for a turbulent reacting liquid flow. Furthermore, most of the previous SGS models for turbulent reacting air flows have been compared only with the DNS under ideal flow and reaction conditions but not with the measurements. It should also be emphasized that it is most desirable to compare the LES results directly with the measurements to examine the credibility of the SGS models.

The purpose of this study is, therefore, to develop the LES with simple algebraic SGS models that are easily applicable to a turbulent reacting liquid flow with the high Schmidt number, and to examine the LES by directly comparing with measurements.

Governing Equations for Large-Eddy Simulation

By applying a filter operation with a filter width $\overline{\Delta}$, the filtered continuity, momentum, and mass conservation equations can be written as follows:

$$\frac{\partial \overline{U_i}}{\partial x_i} = 0 \tag{1}$$

$$\frac{\partial \overline{U_i}}{\partial t} + \frac{\partial \overline{U_j}\,\overline{U_i}}{\partial x_j} = -\frac{\partial \bar{P}}{\partial x_i} + \frac{1}{\mathrm{Re}}\frac{\partial^2 \overline{U_i}}{\partial x_j \partial x_j} - \frac{\partial \tau_{ij}}{\partial x_j} \tag{2}$$

$$\frac{\partial \overline{\Gamma_i}}{\partial t} + \frac{\partial \overline{U_j}\,\overline{\Gamma_i}}{\partial x_j} = \frac{1}{\mathrm{Re\,Sc}}\frac{\partial^2 \overline{\Gamma_i}}{\partial x_j \partial x_j} - \frac{\partial q_{ij}}{\partial x_j} \pm \bar{\omega} \tag{3}$$

$$\tau_{ij} = \overline{U_i U_j} - \overline{U_i}\,\overline{U_j} \tag{4}$$

$$q_{ij} = \overline{\Gamma_i U_j} - \overline{\Gamma_i}\,\overline{U_j} \tag{5}$$

where the overbar denotes the filtered value, U_i is the velocity vector, Γ_i is the concentration of the chemical species i, and P

is the pressure. The dimensionless parameters appearing in the governing equations are the Reynolds number (Re) and the Schmidt number (Sc). When a second-order, irreversible, and isothermal reaction (A + B $\rightarrow$ P) is considered, the filtered reaction source term is expressed as

$$\bar{\omega} = \mathrm{Da}\overline{\Gamma_A \Gamma_B} \tag{6}$$

where Da is the Damköhler number.

The effects of the unresolved SGS in the above filtered equations for the LES appear in the SGS stress term τ_{ij}, SGS mass flux term q_{ij}, and filtered reaction source term ω. These terms need to be modeled to represent the effects of the SGS by the filtered quantities at the resolved grid-scales (GS). Several models such as the Smagorinsky model (Smagorinsky, 1963), dynamic subgrid-scale models (Germano et al., 1991; Lilly, 1992; Piomelli and Liu, 1995), and dynamic mixed subgrid-scale models (Salvetti and Banajee, 1995; Zang et al., 1993) have been proposed for the SGS stresses and mass fluxes. However, an appropriate model for the filtered reaction source term $\bar{\omega}$ has not been proposed especially for a turbulent reacting liquid flow. Thus, it is of great importance to propose a simple and credible SGS model for $\bar{\omega}$ that is applicable to a turbulent reacting liquid flow.

SGS Modeling for a Rapid Reaction

The timescale of the chemical reaction τ_c is defined by

$$\tau_c = \frac{1}{k_r \sqrt{\Gamma_{A0}\Gamma_{B0}}} \tag{7}$$

and in the rapid reaction case the timescale is far smaller than that of the turbulent diffusion τ_t, which is defined by

$$\tau_t = \frac{l_I}{\sqrt{\langle q^2 \rangle}} \tag{8}$$

Here, l_I is the integral length scale, $\langle q^2 \rangle$ is the turbulence kinetic energy and k_r is the reaction rate constant. Γ_{A0} and Γ_{B0} are the initial concentrations of the chemical species A and B. The time step Δt for integrating Eqs. 2 and 3 in the moderately fast reaction case must be selected to satisfy the condition of the Courant number smaller than unity. On the other hand, Δt in the rapid reaction case must be sufficiently smaller than the very small timescale of the chemical reaction τ_c. However, such a small time step cannot be set even for the fastest supercomputer. Therefore, the SGS model of Cook and Riley (1994) for the conserved scalar was applied for the rapid reaction case.

Subtracting the mass conservation equation of species B from that of species A, with the assumption of equal molecular diffusivities, the reaction source term is eliminated so that the conserved scalar Z, which is an invariable parameter irrespective of a chemical reaction, is obtained. The conserved scalar Z is defined by

$$Z = \Gamma_A - \Gamma_B \tag{9}$$

The conserved scalar can be normalized in the form

$$\zeta = \frac{Z - Z_{B0}}{Z_{A0} - Z_{B0}} \tag{10}$$

where Z_{A0} and Z_{B0} are the initial values given by $Z_{A0} = \Gamma_{A0}$ and $Z_{B0} = -\Gamma_{B0}$.

The conservation equation of the filtered ζ is

$$\frac{\partial \bar{\zeta}}{\partial t} + \frac{\partial \overline{U_i}\,\bar{\zeta}}{\partial x_j} = \frac{1}{\mathrm{Re\,Sc}} \frac{\partial^2 \bar{\zeta}}{\partial x_j \partial x_j} - \frac{\partial q_j}{\partial x_j} \tag{11}$$

where $q_j = \overline{U_j \zeta} - \overline{U_j}\,\bar{\zeta}$.

Assuming the equilibrium chemistry, the concentrations of all species in a nonpremixed, single-step reaction can be directly related to ζ, as follows

$$\Gamma_A(\zeta) = \begin{cases} 0 & (\zeta \le \zeta_{st}) \\ \dfrac{\zeta - \zeta_{st}}{1 - \zeta_{st}} & (\zeta > \zeta_{st}) \end{cases} \tag{12}$$

$$\Gamma_B(\zeta) = \begin{cases} -\dfrac{\zeta - \zeta_{st}}{\zeta_{st}} & (\zeta \le \zeta_{st}) \\ 0 & (\zeta > \zeta_{st}) \end{cases} \tag{13}$$

$$\Gamma_P(\zeta) = \begin{cases} \dfrac{\zeta}{\zeta_{st}} & (\zeta \le \zeta_{st}) \\ \dfrac{1 - \zeta}{1 - \zeta_{st}} & (\zeta > \zeta_{st}) \end{cases} \tag{14}$$

where

$$\zeta_{st} = \frac{\Gamma_{B0}}{\Gamma_{A0} + \Gamma_{B0}} \tag{15}$$

When the filtered ζ is substituted into the above relations between the concentration Γ_i and conserved scalar ζ, the GS concentrations in Eqs. 12–14 result in the primitive case in which the mixing of the chemical species at the SGS is neglected. The GS concentration of Γ_i including SGS mixing should be computed from the probability density function of ζ at the SGS (SGS–PDF) by

$$\overline{\Gamma_i} = \int_0^1 \Gamma_i(\zeta)\, P(\zeta)\, d\zeta \tag{16}$$

Strictly, $P(\zeta)$ should be obtained by solving the PDF equation, but $P(\zeta)$ was here assumed to follow a beta distribution to save the computational time for the LES

$$P(\zeta) = \frac{\zeta^{a-1}(1 - \zeta)^{b-1}}{B(a, b)} \tag{17}$$

where

$$a = \bar{\zeta}\left[\frac{\bar{\zeta}(1 - \bar{\zeta})}{\overline{\zeta'^2}} - 1\right] \qquad b = (a/\bar{\zeta}) - a \tag{18}$$

$$B(a, b) = \int_0^1 \zeta^{a-1}(1-\zeta)^{b-1} d\zeta \tag{19}$$

The accuracy of the beta-PDF model was confirmed by Cook and Riley (1994). The SGS variance of ζ ($\overline{\zeta'^2}$) cannot be obtained from the filtered ζ conservation equation (Eq. 11). By assuming that the small-scale statistics can be inferred from larger-scale statistics, Cook and Riley (1994) proposed a scale similarity model for $\overline{\zeta'^2}$ as

$$\overline{\zeta'^2} \approx c_f \widetilde{\zeta'^2} = c_f(\widetilde{\bar{\zeta}^2} - \tilde{\bar{\zeta}}^2) \tag{20}$$

where $\tilde{}$ denotes the test-filtered value, which is computable by applying the test filter. Here we used $2\bar{\Delta}$ as a test-filter width.

SGS Modeling for a Moderately Fast Reaction

Filtered reaction source term

In the moderately fast reaction case, the timescale of the chemical reaction is equivalent to that of the turbulent diffusion, so that the mass conservation equation can be calculated by applying an adequate SGS model for the filtered reaction source term. The filtered reaction source term $\mathrm{Da}\,\overline{\Gamma_A \Gamma_B}$ can be decomposed into two terms, as follows

$$\mathrm{Da}\overline{\Gamma_A \Gamma_B} = \mathrm{Da}(\overline{\Gamma_A}\,\overline{\Gamma_B} + \overline{\gamma_A' \gamma_B'}) \tag{21}$$

where γ_i' is the SGS fluctuation of the chemical species i.

A primitive model that neglects the SGS mixing gives the filtered reaction source term

$$\mathrm{Da}\overline{\Gamma_A \Gamma_B} = \mathrm{Da}\overline{\Gamma_A}\,\overline{\Gamma_B} \tag{22}$$

The primitive model cannot accurately calculate the filtered reaction source term when the two chemical species are not completely mixed ($\overline{\gamma_i'^2} \neq 0$).

In this study, we derive the model that involves the mixing of the chemical species at the SGS by using the joint probability density function $P(\Gamma_A \Gamma_B)$ as

$$\mathrm{Da}\,\overline{\Gamma_A \Gamma_B} = \mathrm{Da} \int_0^1 \int_0^1 \Gamma_A \Gamma_B P(\Gamma_A \Gamma_B) d\Gamma_A d\Gamma_B \tag{23}$$

To eliminate one parameter Γ_B, the $P(\Gamma_A \Gamma_B)$ is decomposed into the conditional probability density function of Γ_B for a given Γ_A, $P(\Gamma_B \,|\, \Gamma_A)$, and probability density function of Γ_A, $P(\Gamma_A)$, as follows

$$P(\Gamma_A \Gamma_B) = P(\Gamma_B | \Gamma_A)\, P(\Gamma_A) \tag{24}$$

By substituting Eq. 24 into Eq. 23, the filtered reaction source term can be represented by

$$\mathrm{Da}\overline{\Gamma_A \Gamma_B} = \mathrm{Da} \int_0^1 P(\Gamma_A) < \Gamma_A \Gamma_B | \Gamma_A > d\Gamma_A \tag{25}$$

where $\langle \Gamma_A \Gamma_B \,|\, \Gamma_A \rangle$ is the conditional expectation of the product of species A and B for a given Γ_A. In this equation, the filtered reaction source term $\mathrm{Da}\,\overline{\Gamma_A \Gamma_B}$ can be calculated by giving appropriate models for $P(\Gamma_A)$ and $\langle \Gamma_A \Gamma_B \,|\, \Gamma_A \rangle$. Of course, $P(\Gamma_A)$ and $\langle \Gamma_A \Gamma_B \,|\, \Gamma_A \rangle$ will be obtained by solving the transport equations of the PDF of Γ_A and joint PDF of Γ_A and Γ_B. However, it is not so easy to solve the transport equations for a practical three-dimensional reacting flow. Therefore, in this study, we tried to develop simple models for $P(\Gamma_A)$ and $\langle \Gamma_A \Gamma_B \,|\, \Gamma_A \rangle$. For $P(\Gamma_A)$, we used the beta-PDF model as well as in the rapid reaction case

$$P(\Gamma_A) = \frac{\Gamma_A^{a-1}(1-\Gamma_A)^{b-1}}{B(a, b)} \tag{26}$$

where

$$a = \overline{\Gamma_A}\left[\frac{\overline{\Gamma_A}(1-\overline{\Gamma_A})}{\overline{\gamma_A'^2}} - 1\right] \qquad b = (a/\overline{\Gamma_A}) - a \tag{27}$$

$$B(a, b) = \int_0^1 \Gamma_A^{a-1}(1-\Gamma_A)^{b-1} d\Gamma_A \tag{28}$$

For $\langle \Gamma_A \Gamma_B \,|\, \Gamma_A \rangle$, no model has been developed. Therefore, it is an important subject to propose an appropriate algebraic model for $\langle \Gamma_A \Gamma_B \,|\, \Gamma_A \rangle$ that can be applied to the LES with the low computation cost. We attempt to model the $\langle \Gamma_A \Gamma_B \,|\, \Gamma_A \rangle$ by using the filtered data of DNS obtained in the next section.

Direct numerical simulation for making the database of SGS concentration statistics

To apply the direct numerical simulation to turbulent velocity and concentration fields the computational grid size must be smaller than the smallest length scales of the turbulent velocity and concentration fields and the computational domain must be sufficiently larger than the integral length scales of the turbulent fields. In particular the smallest concentration scale (the Batchelor scale) is about 25 times smaller in a liquid flow with a high Schmidt number than the smallest velocity scale (the Kolmogorov scale). It is thus very difficult to compute a practical reacting liquid flow by means of the conventional DNS. To avoid the problem and to obtain the SGS concentration fluctuation data we performed the DNS for stationary isotropic reacting turbulence in a small computational domain. In this DNS the initial turbulence energy quickly dissipated because eddy sizes in the computational domain were smaller than energy-containing eddies. To maintain statistically stationary velocity fields the constant turbulence energy was added to the velocity field at low wavenumbers. This procedure causes the simulations to reach a quasi-equilibrium state where the turbulence energy dissipated at the small scales is equal to the turbulence energy input at the large scales. The stationary isotropic turbulence can be maintained by using a force that keeps the total turbulence energy E_1 and E_2 in each of the first two wavenumber shells ($1 \leq k < 2$ and $2 \leq k < 3$) constant in time. Here the ratio of E_1 to E_2 was determined to be consistent with the $k^{-5/3}$ law. The details of the technique of

the forcing are described in Chen et al. (1993). Only a different point from Chen et al.'s simulation is that, because of the limitation of the computer's memory, the governing equations were discretized in a real space in this study.

The present computational domain was the cube of $8\pi\times 8\pi\times 8\pi$ mm. The numbers of the grid points were $512\times 512\times 512$. The computational grid width was smaller than the scalar dissipation scale. This grid resolution was practically enough to compute the turbulence statistics as discussed later. The governing equations for a turbulent reacting flow are written as

$$\frac{\partial U_i}{\partial x_i}=0 \tag{29}$$

$$\frac{\partial U_i}{\partial t}+\frac{\partial U_jU_i}{\partial x_j}=-\frac{\partial P}{\partial x_i}+\frac{1}{\mathrm{Re}}\frac{\partial^2 U_i}{\partial x_j\partial x_j} \tag{30}$$

$$\frac{\partial \Gamma_i}{\partial t}+\frac{\partial U_j\Gamma_i}{\partial x_j}=\frac{1}{\mathrm{Re\,Sc}}\frac{\partial^2\Gamma_i}{\partial x_j\partial x_j}\pm \mathrm{Da}\,\Gamma_A\Gamma_B \tag{31}$$

where all quantities were nondimensionalized by the domain size ($L=8\pi$ mm), rms value of the velocity fluctuation ($u_0=0.01$ m/s), density, and initial concentration of species A. The Schmidt number was set to 600. The Reynolds number, based on the microscale, was 22.5 in the DNS. The governing equations were discretized to construct the finite-difference formulations. The spatial derivatives appeared in the N-S and mass conservation equations were approximated by a second-order central difference scheme. The time integrations of the N-S and mass conservation equations were carried out by a second-order Runge–Kutta method. These equations were numerically solved by the fractional step method. The dimensionless time step Δt was set to 1.0×10^{-3}, which was far smaller than the Kolmogorov and Batchelor timescales.

The reaction presumed here was the moderately fast reaction. Following the measurements by Komori et al. (1994), the saponification reaction between sodium hydroxide (NaOH: species A) and methylformate ($HCOOCH_3$: species B) was assumed

$$\mathrm{NaOH}+\mathrm{HCOOCH_3}\rightarrow \mathrm{HCOONa}+\mathrm{CH_3OH} \tag{32}$$

Initial concentrations of two species were 100 mol/m^3. The reaction rate constant k_r was 0.02 m^3/(mol s). Species A and B (species A in the lower stream and species B in the upper stream) were introduced separately into lower and upper parts in the computational domain as an initial condition.

To propose the SGS model for $\langle\Gamma_A\Gamma_B\,|\,\Gamma_A\rangle$ in Eq. 25 by using the data obtained by the above DNS, the LES grids, which consist of $8\times 8\times 8$ grid points, were assumed in the computational domain used for the DNS. Each point for the LES grids was composed of a box average of $64\times 64\times 64$ points for the DNS grids, and the grid width for the LES corresponded to the width within the inertial subrange. The DNS data at dimensionless time $t=1$, when the turbulence was fully developed, were used for modeling the SGS conditional expectation $\langle\Gamma_A\Gamma_B\,|\,\Gamma_A\rangle$.

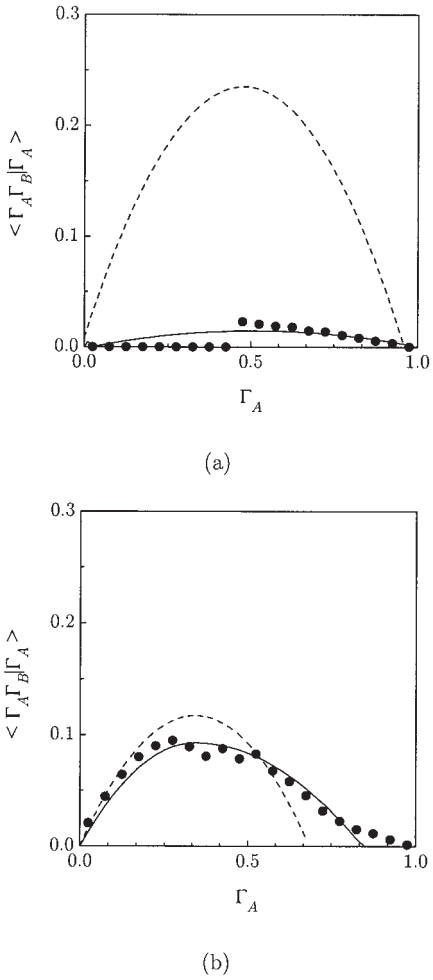

Figure 1. Comparisons of the SGS conditional expectation between the DNS and the present SGS models for two cases.

(a) Very low concentration of the chemical species B at the SGS ($\overline{\Gamma_A}=0.945$, $\overline{\Gamma_P}=5.20\times 10^{-2}$, $=4.66\times 10^{-3}$) and (b) large concentration fluctuation of the chemical product P at the SGS ($\overline{\Gamma_A}=0.425$, $\overline{\Gamma_P}=0.322$, $\overline{\gamma'^2_P}=2.24\times 10^{-2}$). ●, DNS; – – –, Eq. 34; —, Eq. 35.

SGS model for the filtered reaction source term

The SGS conditional expectation $\langle\Gamma_A\Gamma_B\,|\,\Gamma_A\rangle$ of the product of Γ_A and Γ_B for a given Γ_A was modeled as follows. The preservation rule of the dimensionless concentration is presented by

$$\Gamma_A+\Gamma_B+\Gamma_P=1 \tag{33}$$

Assuming that the concentration variance $\overline{\gamma'^2_P}$ of the chemical product P at the SGS is zero (that is, $\Gamma_P=\overline{\Gamma_P}$), the expression for $\langle\Gamma_A\Gamma_B\,|\,\Gamma_A\rangle$ is derived from Eq. 33 as

$$\langle\Gamma_A\Gamma_B|\Gamma_A\rangle=-\left(\Gamma_A-\frac{1-\overline{\Gamma_P}}{2}\right)^2+\frac{1}{4}(1-\overline{\Gamma_P})^2 \tag{34}$$

Figure 1 compares the exact values of $\langle\Gamma_A\Gamma_B\,|\,\Gamma_A\rangle$ obtained from the DNS data (●) with $\langle\Gamma_A\Gamma_B\,|\,\Gamma_A\rangle$ by Eq. 34 (a dotted

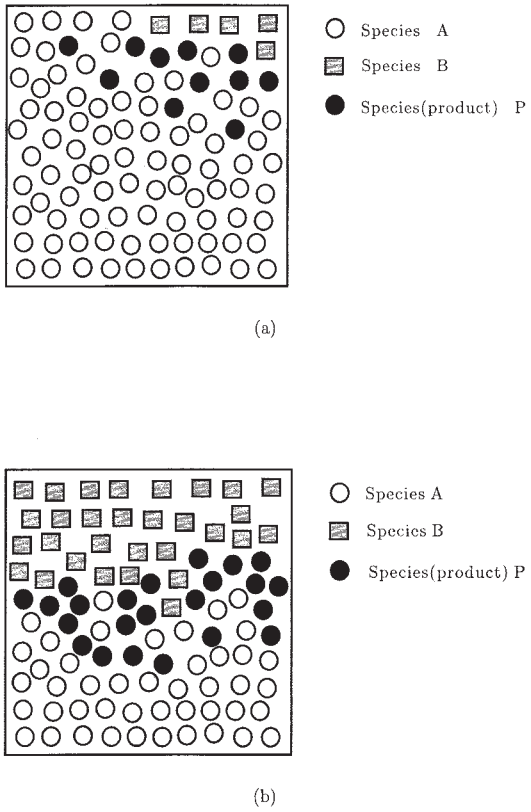

Figure 2. Sketch of the distributions of the chemical species in a LES grid cell for two cases.

(a) Very low concentration of the chemical species B at the GS and (b) large concentration fluctuation of the chemical product P at the SGS.

line). The values by Eq. 34, based on the assumption of $\overline{\gamma'^2_P} = 0$, remarkably deviate from the exact values from the DNS. To obtain good agreement with the exact DNS values, we introduced two parameters α and β into Eq. 34 as

$$\langle \Gamma_A \Gamma_B | \Gamma_A \rangle = \alpha \left\{ -\beta \left(\Gamma_A - \frac{1 - \overline{\Gamma_P}}{2} \right)^2 + \frac{1}{4} (1 - \overline{\Gamma_P})^2 \right\} \tag{35}$$

Here, α ($0 \le \alpha \le 1$) has sufficient influence to reduce Eq. 34 within all areas of Γ_A ($0 \le \Gamma_A \le 1$). The parameter becomes effective when the amount of the chemical species A or B is very small in one grid cell for the LES or the SGS concentration variance of the chemical product P, $\overline{\gamma'^2_P}$, is very large. To consider these two mixing cases, the parameter α was decomposed into the parameters α_1 and α_2, as follows

$$\alpha = \alpha_1 \alpha_2 \tag{36}$$

As the first case, we suppose that a small amount of the chemical species A or B exists in one LES grid cell. Figure 2a shows the distribution of chemical species under the condition that only a small amount of the chemical species B exists in one LES grid cell. In this case, the exact value of $\langle \Gamma_A \Gamma_B | \Gamma_A \rangle$ becomes much smaller than Eq. 34 for all values of Γ_A, given since species A and B can hardly coexist. From the DNS data, this effect was expressed as

$$\alpha_1 = \begin{cases} -(\overline{\Gamma_A} - 1.0)^{16} + 1.0 & (\overline{\Gamma_A} \le \overline{\Gamma_B}) \\ -(\overline{\Gamma_B} - 1.0)^{16} + 1.0 & (\overline{\Gamma_B} \le \overline{\Gamma_A}) \end{cases} \tag{37}$$

The second case is the condition that an abundance of the product P exists near the interface where the reaction occurs as shown in Figure 2b. Chemical species A and B are blocked by the chemical product P at the interface and this situation corresponds to the large concentration variance $\overline{\gamma'^2_P}$ of the chemical product P at the SGS. As a result, the concentration variance of the product P is large, and the value of $\langle \Gamma_A \Gamma_B | \Gamma_A \rangle$ becomes smaller than Eq. 34. It was found from the DNS data that the effect on $\langle \Gamma_A \Gamma_B | \Gamma_A \rangle$ is expressed with a coefficient of $C_\alpha = 0.2$ by

$$\alpha_2 = \frac{0.25(1.0 - \overline{\Gamma_P})^2 - C_\alpha \sqrt{\overline{\overline{\gamma'^2_P}}}}{0.25(1.0 - \overline{\Gamma_P})^2} \tag{38}$$

However, in the region where $\Gamma_A \Gamma_B$ is small (Γ_A is close to 0 or 1) the concentration of the chemical product P is smaller than the GS concentration of the product $\overline{\Gamma_P}$ and the chemical product scarcely coexists with the A and B species. This makes $\langle \Gamma_A \Gamma_B | \Gamma_A \rangle$ a little larger than Eq. 34. From the DNS data, this effect was expressed as

$$\beta = \left\{ 1 - \overline{\Gamma_P} \left[\Gamma_A + \frac{1 + \overline{\Gamma_P}}{2} \right] \right\}^2 \tag{39}$$

Here, $[\cdot]$ denotes the Gauss sign.

These parameters in Eqs. 36–39 have been empirically derived by analyzing the huge DNS data with great effects. If we can theoretically derive the $\langle \Gamma_A \Gamma_B | \Gamma_A \rangle$ through the PDF transport equations, it will be the best way. However, it should be noted that it is very difficult and expensive to derive the $\langle \Gamma_A \Gamma_B | \Gamma_A \rangle$ for a three-dimensional reacting liquid flow by using the PDF method. In this sense, an empirical expression of Eq. 35, derived from the DNS database, is very practical if it can well realize the practical concentration field in a reacting liquid flow.

To examine the present SGS model (Eq. 35) the conditional expectation is compared with the exact values by the DNS in Figure 1. The agreement between two predictions is quite good. Consequently, the $\langle \Gamma_A \Gamma_B | \Gamma_A \rangle$ can well be expressed by substituting Eqs. 36–39 into Eq. 35. The input data to the present SGS model for $\langle \Gamma_A \Gamma_B | \Gamma_A \rangle$ are $\overline{\gamma'^2_P}$, $\overline{\Gamma_A}$, $\overline{\Gamma_B}$, and $\overline{\Gamma_P}$.

The SGS concentration variance $\overline{\gamma_i^2}$ in the SGS models for $\langle \Gamma_A \Gamma_B | \Gamma_A \rangle$ and $P(\Gamma_A)$ (Eqs. 27 and 38) was given by the scale similarity model for $\overline{\gamma_i^2}$ as

$$\overline{\gamma'^2_i} \approx c_f' \widetilde{\gamma'^2_i} = c_f' (\widetilde{\overline{\Gamma_i}^2} - \widetilde{\overline{\Gamma_i}}^2) \tag{40}$$

where c_f' is a correlation coefficient. The terms on the right-hand side are computable in the LES by applying a test filter with a filter width $\tilde{\Delta}$ ($=2\overline{\Delta}$).

Results

Accuracy of the SGS models

Cook and Riley (1994) found the correlation coefficient $c_f' = 1.0$ in Eq. 20 by means of the DNS of a turbulent air flow. However, in a turbulent liquid flow, a viscous-convective subrange in an energy spectrum of concentration fluctuation exists at far smaller scales than the Kolmogorov scale because of the high Schmidt number (Sc $\approx$ 600). The variance of the SGS concentration fluctuation in a liquid flow is thus larger than that in an air flow. As a result, it is expected that the correlation coefficients c_f and c_f' in Eqs. 20 and 40 take values greater than unity.

To determine the appropriate values of c_f and c_f' to a liquid flow case, the same DNS of a stationary isotropic liquid flow was preformed for four Damköhler numbers; no-reaction case of Da = 0 (Case 1), moderately fast reaction cases of Da = 5.0 and 10.0 (Cases 2 and 3), and a rapid reaction case of Da = ∞ (Case 4). In the moderately fast reaction case, a saponification reaction between sodium hydroxide (NaOH: species A) and methylformate ($HCOOCH_3$: species B) was used (see Eq. 32). The two species A and B had the same initial concentration, with values of 100 and 200 mol/m^3 for Da = 5.0 and Da = 10.0, respectively. The reaction rate constant k_r was 0.02 m^3/(mol s). In the rapid reaction case, a neutralization reaction between acetic acid (CH_3COOH: species A) and ammonium hydroxide (NH_4OH: species B) was used

$$CH_3COOH + NH_4OH \rightarrow CH_3COONH_4 + H_2O \quad (41)$$

The initial concentration was 10 mol/m^3 for the two species A and B. The reaction rate constant k_r was 10^8 m^3/(mol s). The other parameters were the same as in the DNS, which was implemented for proposing the present SGS model. The details of the computational conditions are listed in Table 1.

Figure 3 shows the joint probability density functions of the filtered and test-filtered mean-squared concentration fluctuations of the chemical species A for the three cases (Cases 1, 2, and 4). Figure 4 also shows the joint probability density functions of the filtered and test-filtered mean-squared concentration fluctuations of the product P for the moderately fast reaction case (Case 2). The slopes of the lines shown in these figures were determined using a least-squares method and the best-fitting values for the slopes were 5.0 for all cases. Furthermore, to investigate the dependency of the correlation coefficients c_f and c_f' on the Schmidt number Sc, the variations of the c_f and c_f' with Sc for three Damköhler numbers (Da = 0, Da = 5.0, and Da = ∞) were obtained by the above DNS, as shown in Figure 5. The coefficients c_f and c_f' increase with increasing Sc in the range of $1 \leq Sc \leq 50$, whereas they level off at a value of 5.0 in the range of Sc $>$ 50. These plateaus in the range of Sc $>$ 50 can be explained by considering the power spectrum of concentration fluctuation. For a high Schmidt number, the viscous-convective subrange appears in the power spectrum of concentration fluctuation at higher

Table 1. Computational Conditions for the DNS of Stationary Isotropic Liquid Turbulence

Case	Damköhler Number Da	Type of Chemical Reaction
1	0.0	No reaction
2	5.0	Moderately fast reaction
3	10.0	Moderately fast reaction
4	2.5×10^9 ($\approx\infty$)	Rapid reaction

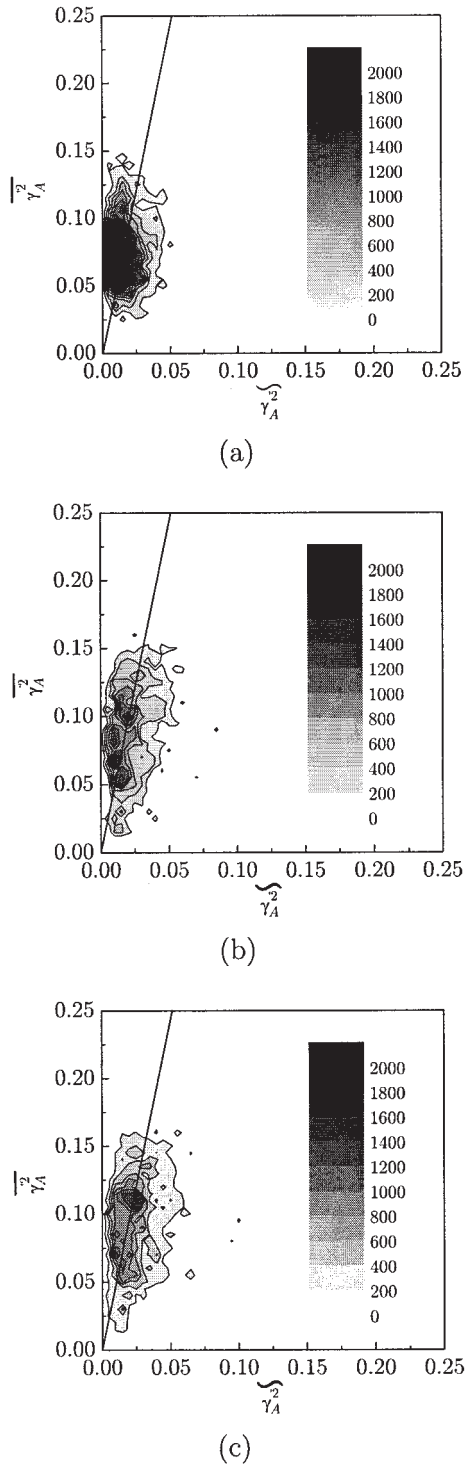

Figure 3. Joint probability density functions of the filtered and test-filtered mean-squared concentration fluctuations of the species A.

(a) In a nonreacting flow (CASE 1); (b) in a reacting flow with a moderately fast reaction (CASE 2); (c) in a reacting flow with a rapid reaction (CASE 4).

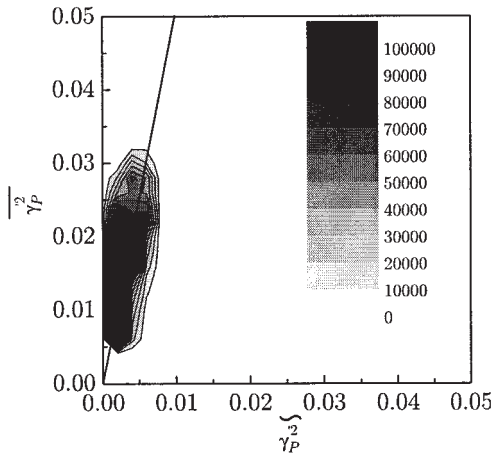

Figure 4. Joint probability density functions of the filtered and test-filtered mean-squared concentration fluctuations of the chemical product P in a reacting flow with a moderately fast reaction (CASE 2).

wavenumbers than at the wavenumbers corresponding to the smallest velocity scale; the Kolmogorov scale. As the Schmidt number increases, the viscous-convective subrange spreads to the higher-wavenumber region and therefore the SGS concentration variance increases. However, because the power spectrum exponentially decreases in the viscous-convective subrange with increasing Schmidt number, the contribution of the spreading viscous-convective subrange to the SGS concentration variance becomes negligibly small at very high wavenumbers and thus the SGS concentration variance approaches a constant value beyond some high Schmidt number. In contrast with the SGS concentration variance, the test-filtered concentration variance has almost the same value irrespective of the Schmidt number, because the effect of the Schmidt number appears at scales smaller than the grid scale. These views of the power spectrum indicate that the correlation coefficients c_f and c_f' in Eqs. 20 and 40 reach a constant value beyond some high Schmidt number. In fact, c_f and c_f' reach a constant value of 5.0 in the region of $Sc \geq 50$, and these values $c_f = c_f' = 5.0$ will be unchanged even for infinite Sc. For different computational grid sizes within the inertial subrange, the same values of c_f and c_f' were also obtained. Here, to verify the accuracy of the above results ($c_f = c_f' = 5.0$), an expensive DNS with Da = 0, by using a finer grid resolution of 1024^3 grids than the present one of 512^3, was performed. The difference in c_f between two DNSs is negligibly small, as shown in Figure 5, and thus it is concluded that the present DNS, with the computational grids smaller than the scalar-dissipation length scale, can accurately obtain turbulent statistics.

To show the applicability of the beta-PDF model for the concentration of chemical reactive species Γ_A, the PDF for Γ_A by the beta-PDF model is compared with the PDF by the DNS for Da = 5.0 (Case 2) in Figure 6. The beta-PDF model for Γ_A is in good agreement with the real PDF obtained by the DNS in the wide range between the well-mixed interfacial region with two chemical species (Figure 6a) and the not well-mixed region outside or near the edge of the interfacial region (Figure 6b). This verifies the applicability of the beta-PDF model to a reacting flow.

To examine the accuracy of the SGS models for a moderately fast reaction, the predictions $\overline{(\Gamma_A\Gamma_B)}_m$ by the present SGS model (Eq. 25 and Eqs. 34–40) should be compared with the exact DNS values $\overline{(\Gamma_A\Gamma_B)}_e$. The comparisons were conducted on all LES grid points for the two cases (Cases 2 and 3) listed in Table 1 to investigate the effects of Da. Figure 7 shows the joint probability density functions of the DNS values $\overline{(\Gamma_A\Gamma_B)}_e$ and the present SGS model predictions $\overline{(\Gamma_A\Gamma_B)}_m$. Although the present model shows a little scattered data, high values of the PDF exist around the 45° line. This means that the agreement between $\overline{(\Gamma_A\Gamma_B)}_m$ and $\overline{(\Gamma_A\Gamma_B)}_e$ is good. It is also found that the present SGS model well predicts the effect of the Damköhler number on $\overline{\Gamma_A\Gamma_B}$. On the other hand, the primitive model overpredicts the value of $\overline{\Gamma_A\Gamma_B}$ on all LES grid points, as shown in Figure 8. This is attributed to the assumption of the perfect mixing of the chemical species at the SGS. The assumption leads the primitive model to the overestimation of the amount of the chemical product.

For a rapid reaction, the predictions $\overline{(\Gamma_P)}_m$ by the present SGS model in Eqs. 12–20 and by the primitive model with $\zeta = \bar{\zeta}$ in Eqs. 12–14 are compared with the exact DNS values $\overline{(\Gamma_P)}_e$ in Figures 9 and 10. The primitive model for the rapid reaction overpredicts the value of the product concentration, whereas the present SGS model shows good agreement with the DNS values. This means that the present SGS model for the rapid reaction is much better than the primitive model.

Large-eddy simulation of a mixing layer liquid flow downstream of a turbulence-generating grid

To confirm whether the present SGS models for both rapid and moderately fast reactions are applicable for a practical turbulent reacting liquid flow, the SGS models should be compared not only with the DNS values, but also with the measurements. Thus, the LES was performed for a reacting mixing-layer liquid flow downstream of a turbulence-generating grid, where Komori et al. (1993a,b, 1994, 1996) measured

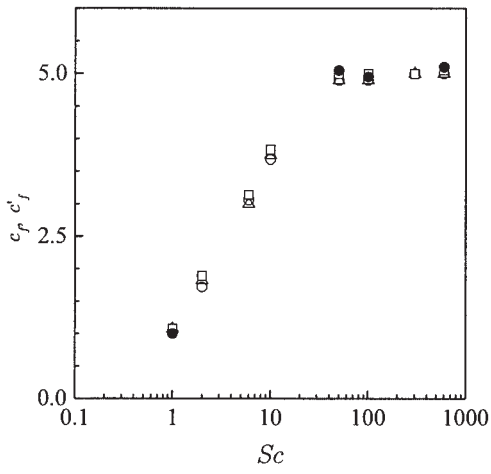

Figure 5. Variations of the c_f and c_f' with the Schmidt number (Sc) for three Damköhler numbers (Da).

○, Da = 0; △, Da = 5.0; □, Da = ∞; ●, Da = 0 with the grid resolution of 1024^3.

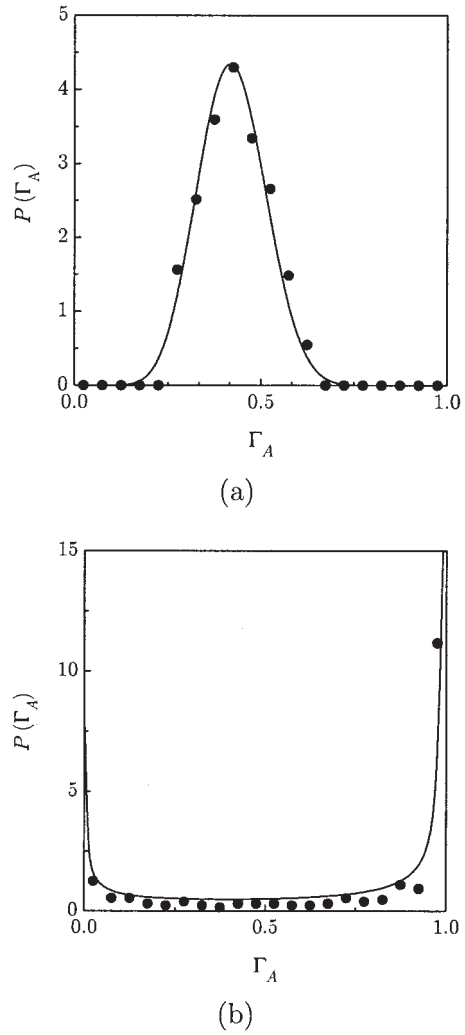

Figure 6. Comparisons of the PDF of Γ_A by the beta-PDF model with that by the DNS under (a) well-mixed conditions and (b) moderately mixed conditions.

●, DNS; —, beta-PDF.

the concentration statistics. Figure 11 shows the schematic diagram of the computational domain. The computational domain was 520 × 80 × 80 mm in streamwise, vertical, and spanwise directions. A turbulence-generating grid, on which the velocity components are set to zero, was located at 2.0×10^{-2} m downstream from the entrance of the computational domain. The mesh size M and thickness of the square rod d were 2.0×10^{-2} m and 2.0×10^{-3} m, respectively. The round-rod grid with a diameter of $d' = 3.0 \times 10^{-3}$ m used in the experiments could not be used in the simulation because of the limitations of the coordinate system and the computer's memory, which can describe the real surface of the round rod. Of course, we experimentally confirmed that the square rod with the thickness of 2.0×10^{-3} m gives the same flow field as in the case of the round rod with the diameter of 3.0×10^{-3} m. The mean streamwise velocity was 0.25 m/s. These flow conditions were identical to those in the experiments by Komori et al. (1991, 1993a,b, 1994). The numbers of the LES grid points used here were 260 × 80 × 80 in the streamwise, vertical, and spanwise directions. The slip boundary conditions were imposed on the velocity components on the upper, lower, and side walls because the computational domain was smaller than the experimental one in Komori et al. (1993a,b, 1994). Species A and B were introduced separately in the lower and upper streams upstream of the turbulence-generating grid.

The governing equations for the LES were given by Eqs. 1–3. All quantities were nondimensionalized using by the grid mesh size M, cross-sectionally averaged velocity U_{ave}, density, and initial concentration of species A. These equations were discretized on a staggered mesh arrangement to construct a

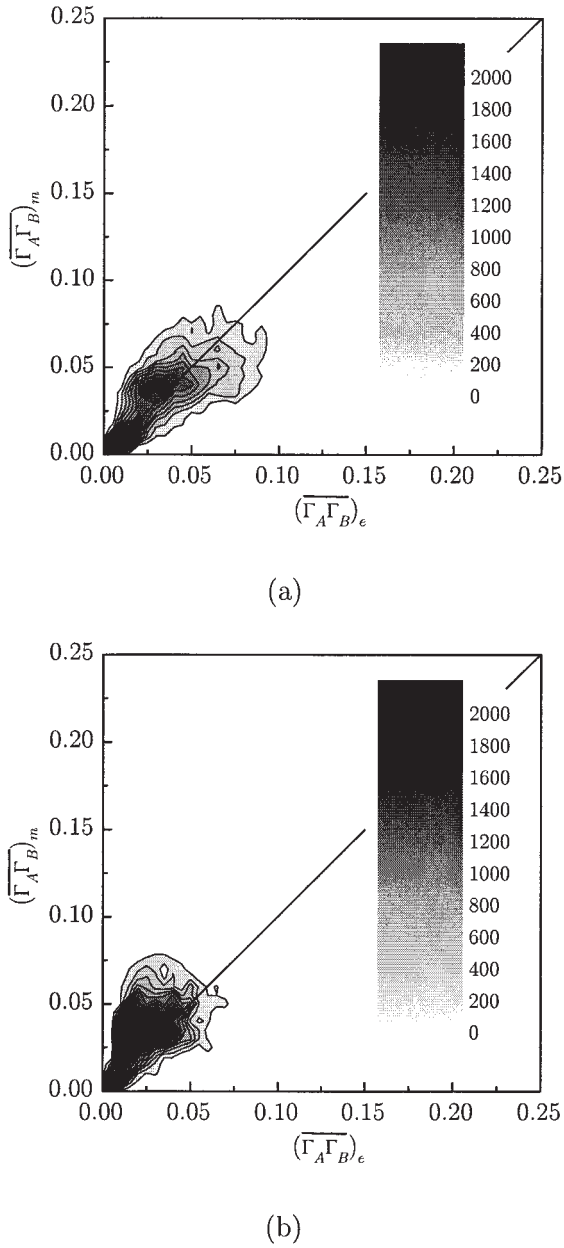

Figure 7. Joint probability density functions of $\overline{\Gamma_A \Gamma_B}$ predicted by the DNS and that by the present SGS model.

(a) Da = 5.0; (b) Da = 10.0.

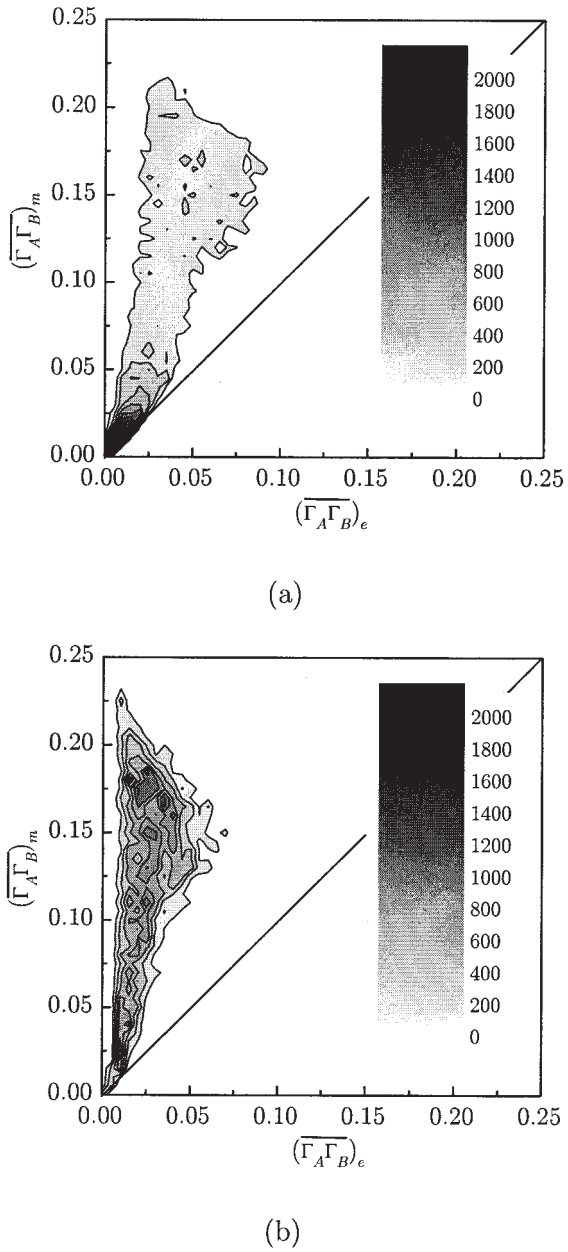

Figure 8. Joint probability density functions of $\overline{\Gamma_A\Gamma_B}$ predicted by the DNS and that predicted by the primitive model.

(a) Da = 5.0; (b) Da = 10.0.

finite-difference formation. The spatial derivatives in the filtered N-S and mass conservation equations were approximated by a second-order central difference scheme. The HSMAC method (Hirt and Cook, 1997) was used to solve the N-S equation. The accuracy of the HSMAC method was confirmed by Nagata and Komori (2001). The time integrations of the N-S and mass conservation equations were carried out by a second-order Runge–Kutta method. The dynamic SGS models were applied for the SGS stresses and SGS mass fluxes. The time step was set to 1.0×10^{-3}. The computations were performed for three reaction conditions: no-reaction, a moderately fast

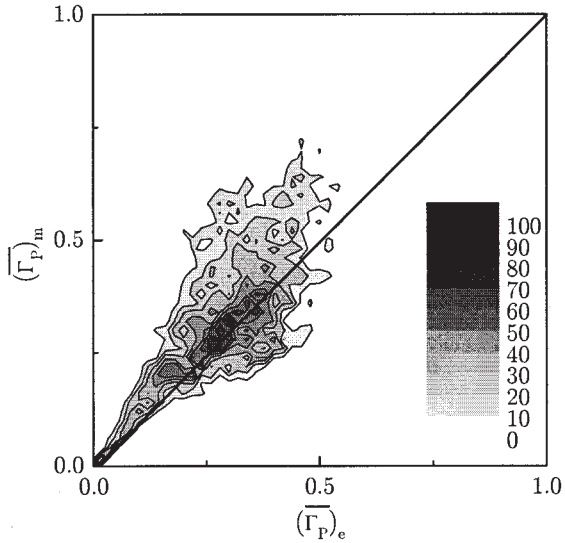

Figure 9. Joint probability density functions of $\overline{\Gamma_P}$ predicted by the DNS and that by the present SGS model for a rapid reaction.

reaction (Eq. 32), and a rapid reaction (Eq. 41), as listed in Table 2.

Figure 12 shows the streamwise distributions of turbulent intensities of the longitudinal and vertical velocity fluctuations. The intensities of the longitudinal and vertical velocity fluctuations are in good agreement with the measurements. Figure 13 shows the streamwise distributions of the normalized Reynolds stress $R_{uv} = \langle uv \rangle / (\sqrt{\langle u^2 \rangle}\sqrt{\langle v^2 \rangle})$. The R_{uv} has a very small value of less than 0.05. These results show that the predicted velocity field well represents the same flow field as that in the experiments by Komori et al. (1993a) and a typical grid-generating turbulence is numerically realized in the LES.

Figure 14 shows the vertical distributions of mean concen-

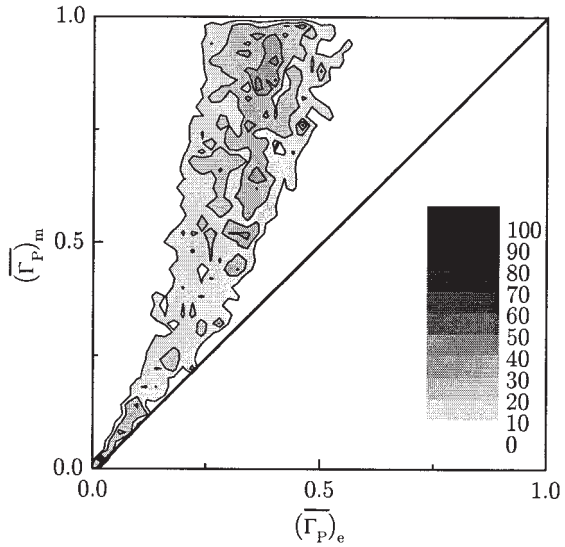

Figure 10. Joint probability density functions of $\overline{\Gamma_P}$ predicted by the DNS and that by the primitive model for a rapid reaction.

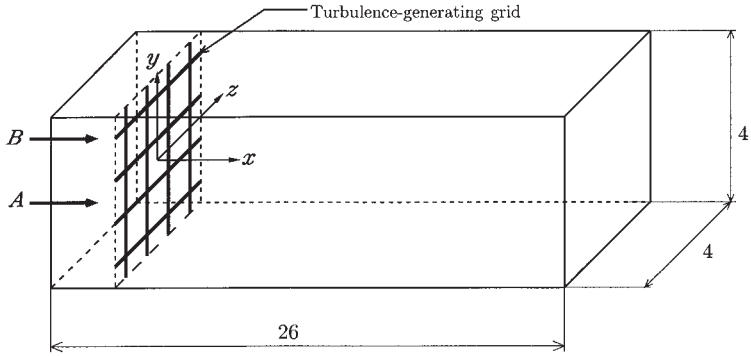

Figure 11. Computational domain.

tration of species A in nonreacting flow at $x = 12$ and 20. Here, x is normalized by the grid-mesh size. The LES predictions of the mean concentration are in good agreement with the measurements in Komori et al. (1993a, 1994). Figure 15 shows the streamwise distributions of mean-squared concentration fluctuation of species A on the centerline ($y = 0$) in a nonreacting flow. The conventional LES takes no account of the effect of the SGS concentration fluctuation on the mean-squared concentration fluctuation, so that the predictions shown by a dotted line in Figure 15 become smaller than the measurements. To include the effect of the SGS concentration fluctuation, a correction method was proposed here.

Figure 16 shows a sketch of time records of the concentrations. The time-averaged squared concentration fluctuation of species A is defined by using $\langle \cdot \rangle$ as

$$\langle \gamma_A^2 \rangle = \langle \Gamma_A^2 \rangle - \langle \Gamma_A \rangle^2 \tag{42}$$

The instantaneous concentration Γ_A, shown by a solid line in Figure 16, cannot be computed by the LES, and therefore two time-averaged terms $\langle \Gamma_A^2 \rangle$ and $\langle \Gamma_A \rangle$ in Eq. 42 are decomposed, as follows

$$\langle \Gamma_A \rangle = \langle \overline{\Gamma_A} \rangle \tag{43}$$

$$\langle \Gamma_A^2 \rangle = \langle \overline{\Gamma_A}^2 \rangle + \langle \gamma'^2_A \rangle \tag{44}$$

Here, $\langle \gamma'_A \rangle$ and $\langle \gamma'_A \overline{\Gamma_A} \rangle$ in Eqs. 43 and 44 are negligibly small, compared to other terms, and the time-averaged concentration $\langle \Gamma_A \rangle$ is equal to the time-averaged filtered concentration $\langle \overline{\Gamma_A} \rangle$. By using the relations in Eqs. 40 and 43, Eq. 44 is transformed to

$$\langle \Gamma_A^2 \rangle = \langle \overline{\Gamma_A}^2 \rangle + \langle \overline{\gamma'^2_A} \rangle = \langle \overline{\Gamma_A}^2 \rangle + c'_f \langle \widetilde{\overline{\Gamma_A}^2} - \widetilde{\overline{\Gamma_A}}^2 \rangle \tag{45}$$

Table 2. Computational Conditions for the LES

Type of Chemical Reaction	Initial Concentrations Γ_{A0}, Γ_{B0} (mol/m^3)	Damköhler Number Da
No reaction	10	0
Moderately fast reaction	100	0.64
Rapid reaction	10	1.6×10^8 ($\approx\infty$)

By substituting Eqs. 43 and 45 into Eq. 42, the time-averaged squared concentration fluctuation, including the effect of the SGS concentration fluctuation, is finally given as

$$\langle \gamma_A^2 \rangle = \langle \overline{\Gamma_A}^2 \rangle - \langle \overline{\Gamma_A} \rangle^2 + c'_f \langle \widetilde{\overline{\Gamma_A}^2} - \widetilde{\overline{\Gamma_A}}^2 \rangle \tag{46}$$

The mean-squared concentration fluctuations corrected by this relation (Eq. 46) are shown by a solid line in Figure 15, and the corrected predictions are in good agreement with the measurements. These results in Figures 14 and 15 show that the present LES can well describe the concentration field in nonreacting grid-generating turbulence.

To examine whether the present SGS models are applicable to a reacting liquid flow, the streamwise distributions of mean concentration of the chemical product P are shown for both a rapid reaction and a moderately fast reaction in Figure 17. Figure 17a shows the results of the LES based on the present SGS models. The predictions by the present SGS models are in good agreement with the measurements. On the other hand, the results of the LES based on the primitive models overpredict the mean concentration of product P for both moderately fast and rapid reaction cases, as shown in Figure 17b.

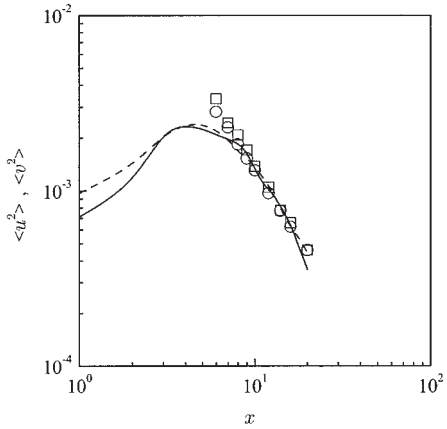

Figure 12. Streamwise distributions of turbulence intensities.

Symbols denote the measurements by Komori et al. (1993b) and the lines are the results of the LES: ○, —, $\langle u^2 \rangle$; □, – – –, $\langle v^2 \rangle$.

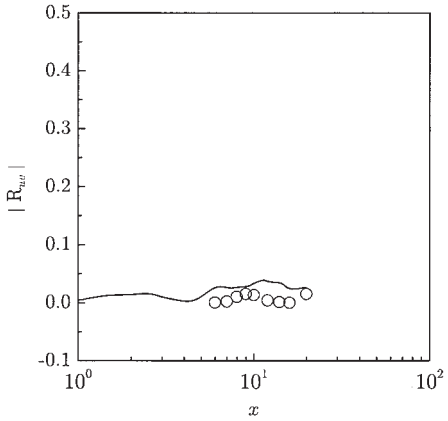

Figure 13. Streamwise distributions of the normalized Reynolds stress.

○, the measurements by Komori et al. (1993b); —, by the LES.

Figure 18 shows the streamwise distributions of mean-squared concentration fluctuation of species A for moderately fast and rapid reaction cases. The corrected method of Eq. 46 gives good agreement with the measurements, compared to the conventional method. The agreement means that the present corrected method well computes the mean-squared concentration fluctuation in turbulent reacting liquid flows.

The results mentioned above suggest that the LES with the present SGS models is very useful for predicting various concentration statistics of a turbulent reacting liquid flow.

Large-eddy simulation of a reacting gas mixing layer

The applicability of the present SGS models to a grid-generating turbulent reacting liquid flow was confirmed through comparison with measurements in the previous subsection. However, the turbulence structure in the grid-generating turbulence without mean shear may be close to stationary isotropic turbulence used in the DNS for making the present SGS models. To show the extensive applicability of the present

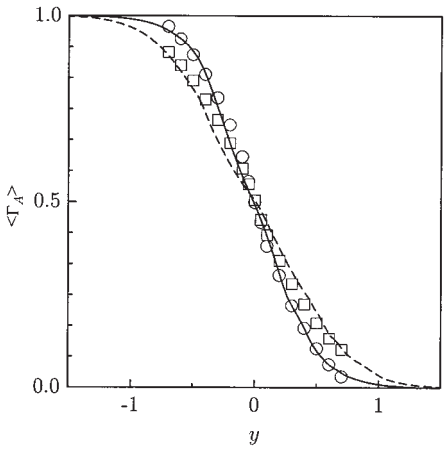

Figure 14. Vertical distributions of mean concentration of species A in a nonreacting flow.

Symbols denote the measurements and the lines are the results of the LES: ○, —, $x = 12$; □, – – –, $x = 20$.

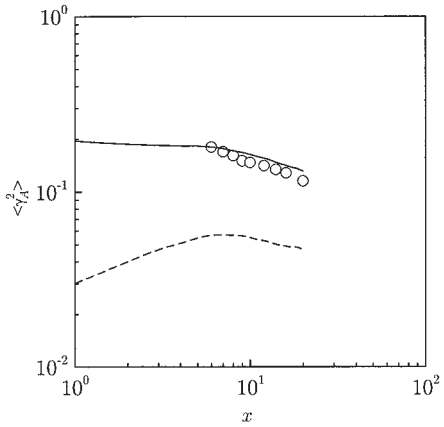

Figure 15. Streamwise distributions of mean-squared concentration fluctuation of species A in a nonreacting flow.

○, measurements by Komori et al. (1993b); – – –, by the conventional LES method; —, by the corrected LES method with the SGS variance.

SGS models, we have to compare the present LES with the measurements in a type of turbulent flow different from the isotropic turbulence. However, at the present stage, we have no reliable measurements of concentration statistics for both moderately fast and rapid reactions in a different type of turbulent flow such as a highly sheared mixing layer because the same measuring technique based on the combination of laser-induced fluorescence and electrode conductivity, as used in Komori et al. (1994), cannot be applied to a highly sheared mixing layer because of the problem of frequency response. Therefore, we tried to compare the present LES predictions with the full DNS predictions of a reacting sheared gas mixing layer with Sc = 1.0, in which the flow structure is far from isotropic turbulence and the full DNS can be performed because of the low Schmidt number.

Figure 19 shows the computational domain for the sheared reacting gas mixing layer. The computational domain was the cube of $4\pi \times 4\pi \times 4\pi$ cm in streamwise, vertical, and spanwise directions. The origin of the coordinate axes x, y, and z was set to the center of the computational domain. The coordinates axes x, y, and z were normalized by the computational domain size $L = 4\pi$ cm. The flow direction of the upper layer was opposite to that of the lower layer and the mean shear was

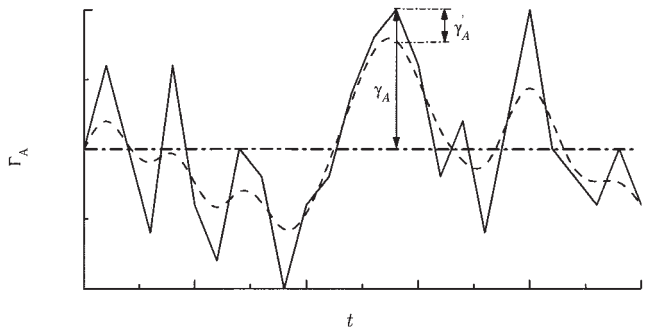

Figure 16. Time records of the concentrations.

—, instanteneous concentration; – – –, filtered concentration; — - —, time-averaged concentration.

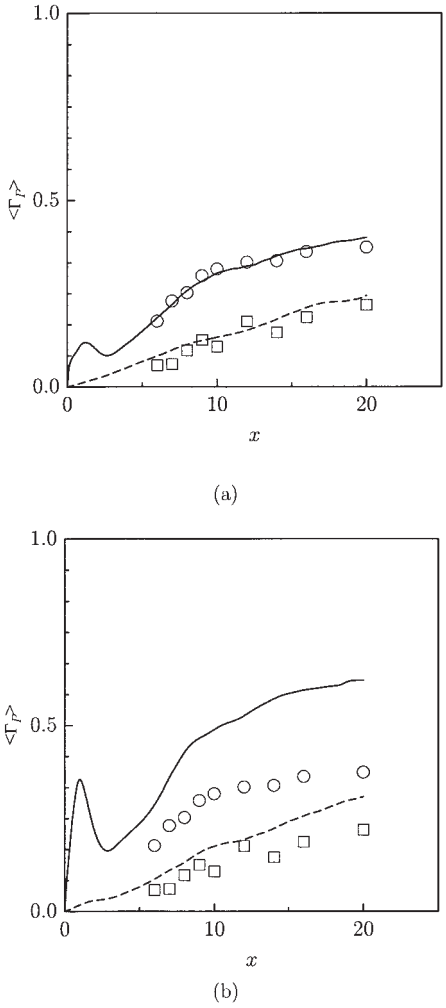

Figure 17. Streamwise distributions of mean concentration of the chemical product P.

Symbols denote the measurements by Komori et al. (1994) and the lines are the results of the LES by (a) the present SGS model with $c_f = c'_f = 5.0$ and (b) the primitive model: ○, —, a rapid reaction; □, – – –, a moderately fast reaction.

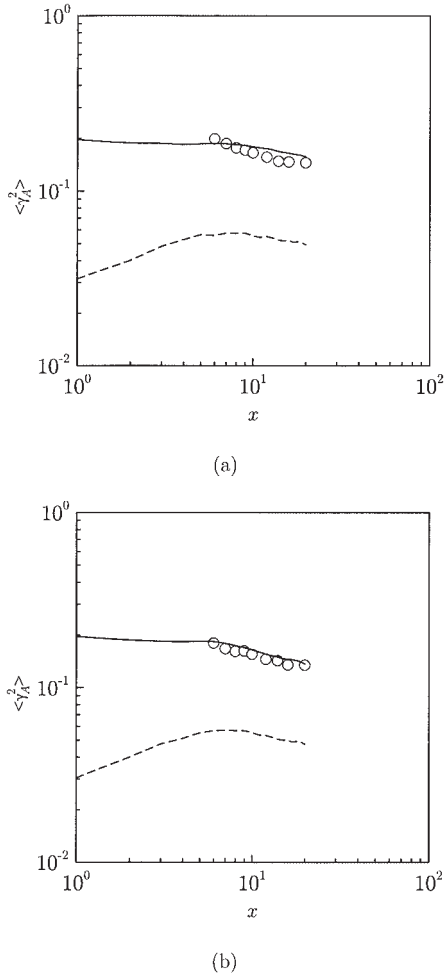

Figure 18. Streamwise distributions of mean-squared concentration fluctuation of the species A in a reacting flow with (a) a rapid reaction and (b) a moderately fast reaction.

Symbols as in Figure 15.

generated by the velocity difference between the counter flows. Chemical species A and B were introduced separately into lower and upper parts in the computational domain at the initial time $t = 0$. Periodic boundary conditions were imposed in the streamwise and spanwise directions, whereas in the vertical direction the top and bottom boundaries were treated as the free slip walls. The numbers of the computational grid points were $256 \times 256 \times 256$ in the x, y, and z directions for the DNS and $32 \times 32 \times 32$ for the LES. The governing equations were Eqs. 29–31 for the DNS and Eqs. 1–3 for the LES. The governing equations were nondimensionalized by the computational domain size ($L = 4\pi$ cm), the streamwise velocity ($U_0 = 2$ m/s), the density, and the initial concentration of species A. The governing equations were solved using the same finite-difference methods used in the DNS and LES in the previous section. For the SGS models in Eqs. 35–39, the same functions of α and β were used and the correlation coefficients in Eqs. 20 and 40, c_f and c'_f, were set to 1.0 for Sc = 1.0 (see Figure 5).

The Reynolds number based on the initial velocity difference and vorticity thickness at $x = 0$ was 3350. Here, the vorticity thickness was defined by $2/(d\langle U \rangle/dy)\,|_{\max}$.

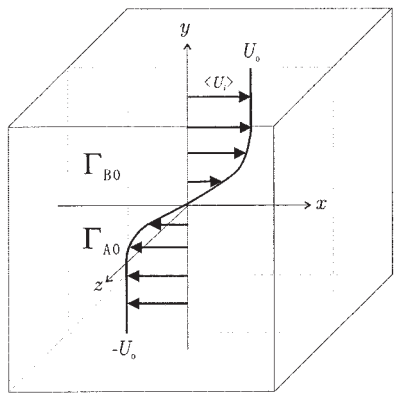

Figure 19. Computational domain for a reacting gas mixing layer.

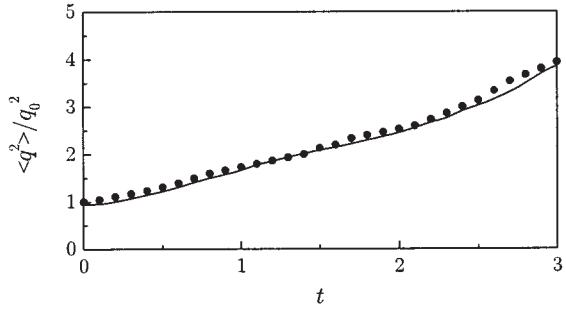

Figure 20. Time evolution of the turbulent kinetic energy.

●, DNS; —, LES with the SGS turbulent kinetic energy.

The hyperbolic tangent velocity profile was used as the initial mean velocity shown in Figure 19

$$\langle U(y) \rangle / U_0 = \tanh(0.5y) \tag{47}$$

The random perturbation u_i was given in the sinusoidal form

$$u_i(x, y, z) = \sum_{n=1}^{20} u_i''(y) \sin[2\pi n f_0 x + \theta_i(x, y, z, nf_0)] \tag{48}$$

$$U_i(x, y, z) = \langle U_i(y) \rangle + u_i(x, y, z) \tag{49}$$

where $u_i''(y)$ is the rms value of the turbulence intensity, f_0 is the basic frequency of 10 Hz, and θ_i is the uniformly distributed random number between 0 and 1. The rms value of the turbulence intensity was given as

$$u_i''(y)/U_0 = 0.10 \exp(-0.147y^2) \tag{50}$$

The temporally growing mixing layer with the periodic boundary conditions was characterized by statistical homogeneity in the x–z plane, and therefore the statistical quantities from the DNS and LES were estimated by taking averages on the x–z plane at a given y.

Figure 20 shows the time evolution of the turbulent kinetic energy in the sheared gas mixing layer at $y = 0$. Here t is normalized by U_0/L. The turbulent kinetic energy is normalized by the initial turbulent kinetic energy q_0^2. It is found that the LES predictions are in good agreement with the DNS predictions. Figure 21 shows the time evolutions of the mean concentration of chemical product P at $y = 0$ for three cases listed in Table 3. Although the LES based on the primitive model in Eq. 22 overestimates the amount of product P, the LES based on the present SGS models well agrees with the DNS as well as in unsheared reacting grid-generating liquid turbulence. Figure 22 shows the time evolution of the mean-squared concentration fluctuation of species A at $y = 0$. The LES predictions based on Eq. 46 are in good agreement with the DNS predictions. These results for a reacting gas mixing layer show that the present SGS models depend on neither flow condition nor the Schmidt number and they are useful for various reacting turbulent flows.

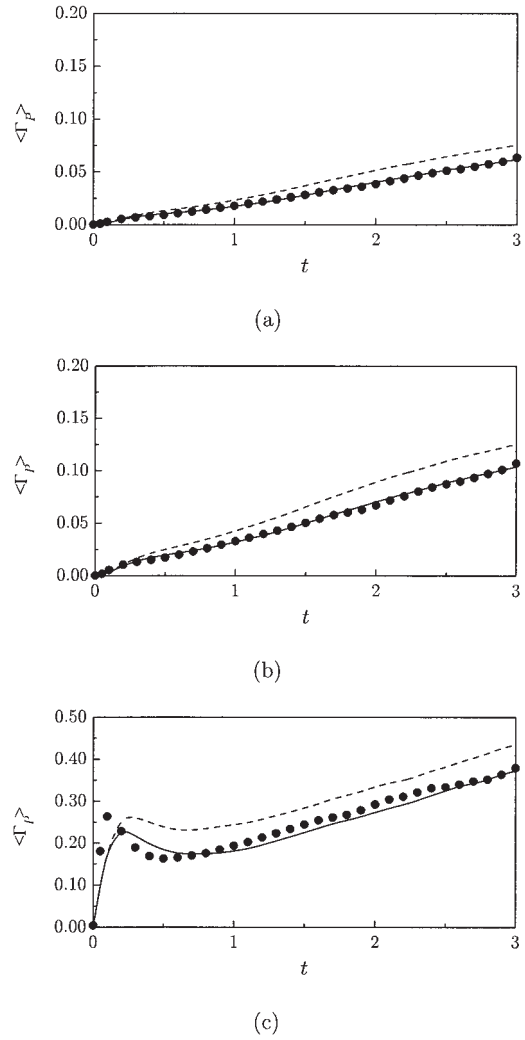

Figure 21. Time evolution of the mean concentration of chemical product P.

(a) In a reacting flow with a moderately fast reaction (CASE 1), (b) in a reacting flow with a moderately fast reaction (CASE 2), and (c) in a reacting flow with a rapid reaction (CASE 3): ●, DNS; —, LES based on the present SGS model; – – –, LES based on the primitive model.

Conclusions

New SGS models for the filtered reaction source term were proposed by using the filtered data obtained from the DNS of a turbulent liquid flow. To examine the SGS models for both rapid and moderately fast reactions, the LES was applied to a

Table 3. Computational Conditions for the DNS and LES of a Reacting Gas Mixing Layer

Case	Reaction Rate Constant [1/(ppm s)]	Γ_{AO} (ppm)	Γ_{BO} (ppm)
1	0.37	10	10
2	0.37	20	20
3	∞	10	10

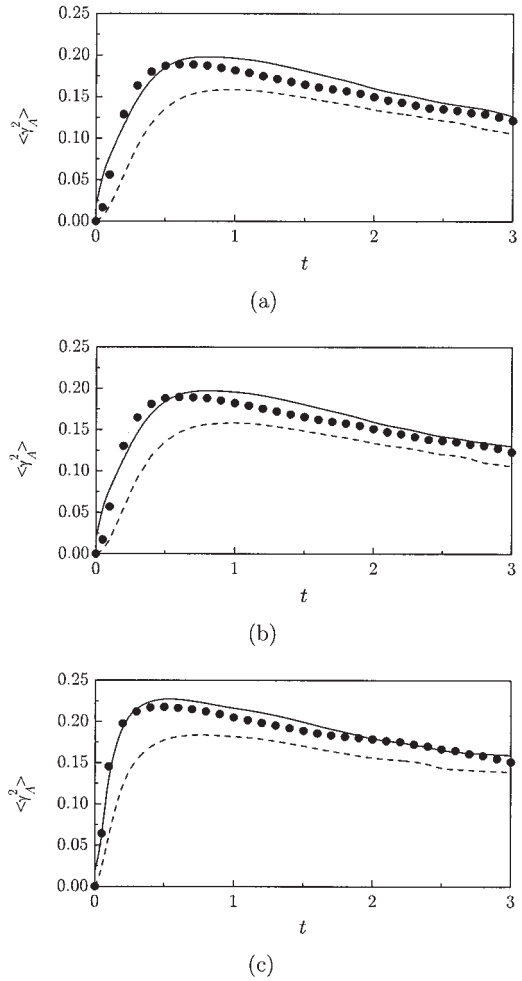

Figure 22. Time evolution of the mean-squared concentration fluctuation of chemical species A.

(a) In a reacting flow with a moderately fast reaction (CASE 1), (b) in a reacting flow with a moderately fast reaction (CASE 2), and (c) in a reacting flow with a rapid reaction (CASE 3): ●, DNS; – – –, by the conventional LES method; —, by the corrected LES method with the SGS variance.

turbulent reacting liquid flow and compared with the measurements. The SGS models were also verified by the DNS of the reacting gas mixing layer. The main results from this study can be summarized as follows.

(1) The present SGS model, which consists of the SGS–PDF and conditional expectation, can well predict the filtered reaction source term for a moderately fast reaction.

(2) The present LES is applicable to both moderately fast and rapid reactions and it can well predict not only the time-averaged concentrations but also the time-averaged squared values of concentration fluctuations in a turbulent reacting flow.

Acknowledgments

This research was supported by the Japanese Ministry of Education, Science and Culture through grants-in-aid (Nos. 14102016 and 15656050) and the 21st Century Center of Excellence Program for Research and Education on Complex Functional Mechanical Systems. This research was also initiated by the Proposal-Based New Industry Creative Technology R&D Promotion Program from the New Energy and Industrial Technology Development Organization (NEDO) of Japan. The LES and DNS were carried out by using a parallel supercomputer of the Center for Global Environment Research, National Institute for Environmental Studies, Environmental Ministry of Japan. The authors also thank Dr. K. Nagata and Mr. R. Onishi for their help.

Notation

$B(a, b)$ = beta function
c_f, c_f' = correlation coefficients in Eq. 20 or Eq. 40 (=5.0: constant)
d = thickness of a square rod
d' = diameter of a round-rod grid
Da = Damköhler number
k_r = chemical reaction rate constant
L = representative length scale
M = mesh size of a turbulent-generating grid
l_I = integral length scale
U_i = velocity vector
u = rms value of the velocity fluctuation
P = pressure
$P(\zeta)$ = probability density function of ζ
$P(\Gamma_i)$ = probability density function of concentration of chemical species i
$\langle q^2 \rangle$ = turbulent kinetic energy
q_{ij} = subgrid-scale mass flux
R_{uv} = normalized Reynolds stress = $\langle uv \rangle / (\sqrt{\langle u^2 \rangle}\sqrt{\langle v^2 \rangle})$
Re = Reynolds number
Sc = Schmidt number
t = time
Z = conserved scalar (= $\Gamma_A - \Gamma_B$)

Greek letters

Γ_i = concentration of the chemical species i
ω = chemical reaction source term
τ_{ij} = subgrid-scale stress
τ_c = timescale of chemical reaction
τ_t = timescale of turbulent diffusion
$\underline{\zeta}$ = normalized conserved scalar = $(Z - Z_{B0})(Z_{A0} - Z_{B0})$
$\underline{\zeta'^2}$ = subgrid-scale valiance of the conserved scalar
$\underline{\gamma_\perp'^2}$ = subgrid-scale valiance of the chemical species i
Δ = computational grid width of the LES
Δt = time step
$\langle \Gamma_A \Gamma_B \,|\, \Gamma_B \rangle$ = conditional expectation of the product of species A and B

Subscripts

A = chemical species A
B = chemical species B
P = chemical production P

Other symbols

$'$ = subgrid-scale fluctuation
$\langle \cdot \rangle$ = time-averaged value
$\underline{\ }$ = filtered value

Literature Cited

Baldyga, J., "A Closure Model for Homogeneous Chemical Reactions," *Chem. Eng. Sci.*, **49**, 1985 (1994).

Bilger, R. W., "Conditional Moment Closure for Turbulent Reacting Flow," *Phys. Fluids A*, **5**, 436 (1993).

Briens, C. L., A. Margaritis, and G. Wild, "A New Stochastic Model and Measurement Errors in Residence Time Distributions of Multiphase Reactors," *Chem. Eng. Sci.*, **50**, 279 (1995).

Bushe, W. K., and H. Steiner, "Conditional Moment Closure for Large Eddy Simulation of Nonpremixed Turbulent Reacting Flows," *Phys. Fluids*, **11**, 1896 (1999).

Chen, S., G. D. Doolen, R. H. Kraichnan, and Z. She, "On Statistical Correlations between Velocity Increments and Locally Averaged Dissipation in Homogeneous Turbulence," *Phys Fluids A*, **5**, 458 (1993).

Colucci, P. J., F. A. Jaberi, P. Givi, and S. B. Pope, "Filtered Density

Function for Large Eddy Simulation of Turbulent Reacting Flows," *Phys Fluids*, **10**, 499 (1998).
Cook, A. W., and J. J. Riley, "A Subgrid Model for Equilibrium Chemistry in Turbulent Flows," *Phys. Fluids*, **6**, 2868 (1994).
Cook, A. W., and J. J. Riley, "Subgrid-Scale Modeling for Turbulent Reacting Flows," *Combust. Flame*, **112**, 593 (1998).
Gao, F., and E. E. O'Brien, "A Large-Eddy Simulation Scheme for Turbulent Reacting Flows," *Phys. Fluids A*, **5**, 1282 (1993).
Germano, M., A. Maffio, S. Sello, and G. Mariotti, "On the Extension of the Dynamic Modeling Procedure to Turbulent Reacting Flows," Proc. of Second ERCOFTAC Workshop on Direct and Large Eddy Simulation, p. 16 (1996).
Germano, M., U. Piomelli, P. Moin, and W. H. Cabot, "A Dynamic Subgrid-Scale Eddy Viscosity Model," *Phys Fluids A*, **3**, 1760 (1991).
Hirt, C. W., and J. L. Cook, "Calculating Three-Dimensional Flows around Structures and over Rough Terrain, " *J. Comp. Phys.*, **10**, 324 (1972).
Jaberi, F. A., P. J. Colucci, S. James, P. Givi, and S. B. Pope, "Filtered Mass Density Function for Large-Eddy Simulation of Turbulent Reacting Flows," *J. Fluid Mech.*, **401**, 85 (1999).
Komori, S., J. C. R. Hunt, T. Kanzaki, and Y. Murakami, "The Effects of Turbulent Mixing on the Correlation between Two Species and on Concentration Fluctuation in Non-Premixed Reacting Flow," *J. Fluid Mech.*, **228**, 629 (1991).
Komori, S., T. Kanzaki, and Y. Murakami, "Concentration Correlation in a Turbulent Mixing layer with Chemical Reactions," *J. Chem. Eng. Jpn.*, **27**(6), 742 (1994).
Komori, S., T. Kanzaki, Y. Murakami, and H. Ueda, "Simultaneous Measurements of Instantaneous Concentrations of Two Species Being Mixed in a Turbulent Flow by Using a Combined Laser-Induced Fluorescence and Laser-Scattering Technique," *Phys. Fluids A*, **1**(2), 349 (1993b).
Komori, S., and K. Nagata, "Effects of Molecular Diffusivities on Counter-Gradient Scalar and Momentum Transfer in Strongly Stable Stratification," *J. Fluid Mech.*, **326**, 205 (1996).
Komori, S., K. Nagata, T. Kanzaki, and Y. Murakami, "Measurements of Mass Flux in a Turbulent Liquid Flow with a Chemical Reaction," *AIChE J.*, **39**(10), 1611 (1993a).
Lilly, D. K., "A Proposed Modification of the Germano Subgrid-Scale Closure Method," *Phys. Fluids A*, **4**, 633 (1992).
Meeder, J. P., and F. T. M. Nieuwstadt, "Large-Eddy Simulation of the Turbulent Dispersion of a Reactive Plume from a Point Source into a Neutral Atmospheric Boundary Layer," *Atmos. Environ.*, **34**, 3563 (2000).
Nagata, K., and S. Komori, "The Difference in Turbulent Diffusion between Active and Passive Scalars in Stable Thermal Stratification," *J. Fluid Mech.*, **430**, 361 (2001).
Patterson, G. K., "Application of Turbulence Fundamentals to Reactor Modeling and Scale-Up," *Chem. Eng. Commun.*, **8**, 25 (1981).
Pierce, C. D., "Progress-Variable Approach for Large-Eddy Simulation of Turbulent Combustion," PhD Thesis, Dept. of Mechanical Engineering, Stanford University, Stanford, CA (2001).
Piomelli, U., and J. Liu, "Large-Eddy Simulation of Rotating Channel Flows Using a Localized Dynamic Model," *Phys. Fluids*, **7**, 839 (1995).
Pitsch, H., and H. Steiner, "Large-Eddy Simulation of a Turbulent Piloted Methane/Air Diffusion Flame (Sandia flame D)," *Phys. Fluids*, **12**, 2541 (2000).
Riley, J. J., R. W. Metcalfe, and S. A. Orszag, "Direct Numerical Simulations of Chemically Reacting Turbulent Mixing Layers," *Phys. Fluids*, **29**, 406 (1986).
Ritchie, B. W., and A. H. Tobgy, "A Three-Environment Micromixing Model for Chemical Reactors with Arbitrary Separate Feedstreams," *Chem. Eng. J.*, **17**, 173 (1979).
Salvetti, M. V., and S. Banerjee, "A Priori Tests of a New Dynamic Subgrid-Scale Model for Finite-Difference Large-Eddy Simulations," *Phys. Fluids*, **7**, 2831 (1995).
Schumann, U., "Large-Eddy Simulation of Turbulent Diffusion with Chemical Reactions in the Convective Boundary Layer," *Atmos. Environ.*, **23**, 1713 (1989).
Smagorinsky, J., "General Circulation Experiments with the Primitive Equations," *Mon. Weather Rev.*, **91**, 99 (1963).
Sykes, R. I., D. S. Henn, S. F. Parker, and W. S. Lewellen, "Large-Eddy Simulation of a Turbulent Reacting Plume," *Atmos. Environ.*, **26A**, 2565 (1992).
Toor, H. L., "Turbulent Mixing of Two Species with and without Chemical Reactions," *Ind. Eng. Chem. Fundam.*, **8**, 655 (1969).
Van Dop, H., "The Evaluation of a Lagrangian Model for Turbulent Transport and Chemistry," *Phys. Fluids*, **13**, 1331 (2001).
Wang, D. M., and J. M. Tarbell, "Closure Models for Turbulent Reacting Flows with a Nonhomogeneous Concentration Field," *Chem. Eng. Sci.*, **48**, 3907 (1993).
Zang, Y., R. L. Street, and J. R. Koseff, "A Dynamic Mixed Subgrid-Scale Model and Its Application to Turbulent Recirculating Flows," *Phys. Fluids A*, **5**, 3186 (1993).

Manuscript received Feb. 3, 2003, and revision received Feb. 23, 2004.